The Astrophysical Journal, 593:L1–L5, 2003 August 10

THE EVOLUTION OF THE GALAXY LUMINOSITY FUNCTION IN THE REST-FRAME BLUE BAND UP TO $z = 3.5$[1]

F. Poli,[2] E. Giallongo,[2] A. Fontana,[2] N. Menci,[2] G. Zamorani,[3] M. Nonino,[4] P. Saracco,[5] E. Vanzella,[6] I. Donnarumma,[2] S. Salimbeni,[2] A. Cimatti,[7] S. Cristiani,[4] E. Daddi,[6] S. D'Odorico,[6] M. Mignoli,[3] L. Pozzetti,[3] and A. Renzini[6]

Received 2003 April 15; accepted 2003 June 30; published 2003 July 16

ABSTRACT

We present an estimate of the cosmological evolution of the field galaxy luminosity function (LF) in the rest-frame 4400 Å B band up to redshift $z = 3.5$. To this purpose, we use a composite sample of 1541 I-selected galaxies selected down to $I_{AB} = 27.2$ and 138 galaxies selected down to $K_{AB} = 25$ from ground-based and *HST* multicolor surveys, most notably the new deep *JHK* images in the Hubble Deep Field–South (HDF-S) taken with the ISAAC instrument at the ESO-VLT telescope. About 21% of the sample has spectroscopic redshifts, and the remaining fraction well-calibrated photometric redshifts. The resulting blue LF shows little density evolution at the faint end with respect to the local values, while at the bright end [$M_B(\mathrm{AB}) < -20$] a brightening increasing with redshift is apparent with respect to the local LF. Hierarchical CDM models overpredict the number of faint galaxies by a factor ~3 at $z \simeq 1$. At the bright end the predicted LFs are in reasonable agreement only at low and intermediate redshifts ($z \simeq 1$) but fail to reproduce the pronounced brightening observed in the high-redshift ($z \sim 2$–3) LF. This brightening could mark the epoch at which major star formation activity is present in the galaxy evolution.

Subject headings: galaxies: distances and redshifts — galaxies: formation

1. INTRODUCTION

The evolution of the luminosity distribution of field galaxies and its correlation with colors constitutes the baseline for studying the link between the stellar processes occurring in galaxies and the dynamical properties of their host dark matter (DM) halos, which are thought to be described by the hierarchical clustering theories. To this aim, observations should (1) sample a wide range of rest-frame wavelengths from the UV down to the optical and NIR bands to derive the contribution of the different stellar populations to the total mass and star formation rate; (2) be extended to faint magnitudes, since feedback effects—regulating the amount of gas that can actually cool and form stars—are effective in depleting the gas content of galaxies in the shallow potential wells, and hence appreciably affect the faint end of the LF; (3) be performed in the same rest-frame band to avoid the mixing (the degeneracy) between redshift- and wavelength-dependent effects, possibly reducing the effect of dust extinction. Fulfilling the above requirements up to high redshifts with a homogeneous sample is not an easy task. At present, the available results are scattered in different bands, depending on z, and have different extensions at faint luminosities.

At $z \approx 0$, recent results in the B band from redshift surveys (Zucca et al. 1997; Folkes et al. 1999; Blanton et al. 2001) have shown that the local population of field galaxies has an LF with a fainter characteristic magnitude and a faint slope steeper than previously found. At intermediate redshifts ($z \simeq 0.75$), spectroscopic surveys (CFRS, Lilly et al. 1995; Autofib, Ellis et al. 1996; CNOC2, Lin et al. 1999) found a steepening of the faint end LF with increasing z in the total LF, mainly due to the contribution by later type galaxies. To investigate the faint end shape and evolution of the LF at higher z, the statistics must be extended well beyond the limit of spectroscopic surveys. The photometric redshift technique (Connolly et al. 1997; Giallongo et al. 1998; Fernandez-Soto, Lanzetta, & Yahil 1999; Fontana et al. 2000) allowed us to obtain a first estimate of the rest-frame B LF at $0 < z < 1.25$ (Poli et al. 2001) using a composite deep multicolor sample in the Hubble Deep Fields (HDF) North and South down to $I_{AB} = 27.2$. The lack of deep NIR images prevented us from following the evolutionary behavior of the LF in the same rest-frame B band to $z > 2$.

In this Letter, we present the results from deep ISAAC/VLT IR data in the HDF-S, which are providing a complete sample of galaxies down to $K_{AB} = 25$, thus giving us the first chance to assess the evolution of the galaxy LF in the same rest-frame 4400 Å B band from redshift $z = 0$ to $z = 3.5$. Throughout this Letter we adopt an $\Omega_\Lambda = 0.7$, $\Omega_M = 0.3$, and $H_0 = 70$ km s^{-1} Mpc^{-1} cosmology.

2. THE DATA SAMPLE

The data set we have analyzed consists of a composite sample of galaxies covering, with similar depth, a range spanning from the UV down to the optical/NIR wavelengths (see Table 1). A first photometric catalog has been extracted from the HDF-S data set, where *HST*/WFPC2 optical images (Casertano et al. 2000) have been combined with deep ESO/VLT NIR images in a 4.22 arcmin^2 sky area (these data are in common with the FIRES survey; Labbé et al. 2003). The infrared images reach formal 5 σ limits in an aperture of 1.″2 at $J_{AB} = 25.3$, $H_{AB} =$

[1] Mainly based on service mode observations collected at the European Southern Observatory, Programme 164.O-0612.

[2] INAF, Osservatorio Astronomico di Roma, via Frascati 33, I-00040 Monteporzio, Italy.
[3] INAF, Osservatorio Astronomico di Bologna, via Ranzani 1, I-40127 Bologna, Italy.
[4] INAF, Osservatorio Astronomico di Trieste, via G.B. Tiepolo 11, I-34131 Trieste, Italy.
[5] INAF, Osservatorio Astronomico di Brera, via Brera, 28, 20121 Milan, Italy.
[6] European Southern Observatory, Karl-Schwarzschild-Strasse 2, D-85748, Garching, Germany.
[7] INAF, Osservatorio Astronomico di Arcetri, Largo E. Fermi 5, I-50125, Florence, Italy.

TABLE 1
THE COMPOSITE SAMPLE

Field	Magnitude Limit	arcmin^2	Filters	N
HDF-S	$I < 27.2$	4.22	*UBVIJHK*	245
HDF-S	$K < 25$	4.22	*UBVIJHK*	113
HDF-N	$I < 27.2$	3.92	*UBVIJHK*	259
HDF-N	$K < 23.5$	3.92	*UBVIJHK*	18
Chandra	$I < 25$	35.6	*UBVRIZJK*	619
Chandra	$K < 21.9$	24.6	*UBVRIZJK*	6
Q0055−269	$I < 24.5$	31.9	*UBGVRR$_W$IZJK*	418
Q0055−269	$K < 21.9$	19.8	*UBGVRR$_W$IZJK*	1

24, and $K_{AB} = 25$. The procedures adopted to extract the final multicolor catalog have been optimized to obtain accurate color photometry for reliable photometric redshifts, as described in Vanzella et al. (2001). The full catalog will be presented in a future paper. From this catalog we have selected 245 $I_{AB} \leq 27.2$ sources to build the LF in the $0.4 < z < 1$ range, and 113 $K_{AB} \leq 25$ sources to sample the LF in the same rest-frame wavelength but at higher redshifts, $1.3 < z < 3.5$. To improve the statistics at the faint end of the LF we added 259 $I_{AB} \leq 27.2$ at $z \leq 1$ and 18 $K_{AB} \leq 23.5$ galaxies at $1.3 < z < 3.5$ from the HDF-N catalog of Fontana et al. (2000). To improve the statistics also at the bright end of the LF, we added a sample of galaxies selected in two fields centered around the QSO 0055−269 and in the *Chandra* Deep Field–South (Giacconi et al. 2001) for a total of $\simeq 68$ arcmin^2, which were used to select the targets for the so-called K20 ($K_{AB} \leq 21.9$) spectroscopic survey (Cimatti et al. 2002a).

Simulations show that the K20 sample and HDFs are complete (to more than 95%) down to $I_{AB} = 24.5$, 25, and 27.2, respectively. Following the procedure presented in Poli et al. (1999), we separately estimate *total* and *color* magnitudes with two different recipes. To obtain the total fluxes of the objects in the chosen reference band, SExtractor Kron magnitudes (Bertin & Arnouts 1996) have been adopted for bright sources. For faint sources we estimated aperture magnitudes with aperture corrections computed estimating the flux losses outside the adopted aperture with respect to the Kron magnitudes for relatively bright sources. The reliability of the correction adopted has been tested by means of simulations as performed in Poli et al. (2001). No appreciable systematic losses of the total flux for the faintest sources were found apart from the well-known losses by 5%–10% typical of the Kron magnitudes. To cope with the inhomogeneous quality of the different images, we produced a set of seeing-corrected *color* magnitudes that have been then scaled to total magnitudes in all the bands (Vanzella et al. 2001). This ensures that colors—used to estimate the redshifts—are measured in the same physical region at any wavelength, independently of the seeing FWHM present in each image.

The final sample includes 1541 *I*-selected and 138 *K*-selected galaxies (see Table 1). Of these, 337 and 23, respectively, have spectroscopic z taken from existing spectroscopic surveys (Cohen et al. for the HDF-N; Vanzella et al. 2002 for the HDF-S; Cimatti et al. 2002a for the K20 sample). For all the other galaxies, reliable photometric redshifts have been derived with a homogeneous technique, described in Fontana et al. (2000) (for the HDF-S sample) and in Cimatti et al. (2002a) (for the K20 survey). The model adopts several galaxy ages and exponentially declining star formation histories and includes Lyman absorption from the intergalactic medium and dust absorption with different amounts up to $E(B-V) = 1$, using both SMC and Calzetti extinction curves. In all the samples, the relative accuracy is $(z_{spe} - z_{phot})/(1 + z_{spe}) \lesssim 0.05$.

3. BUILDING THE OBSERVED LF

Our combined sample allows to probe the behavior of the 4400 Å rest-frame LF in a continuous way from $z \sim 0.4$ up to $z \sim 3.5$. For galaxies at $z < 1$ we used our *I*-band selected sample. Indeed, in the redshift interval $0.7 < z < 1$ the 4400 Å rest-frame wavelength is within the *I* band, and the LF includes all the galaxies with $m[4400(1 + z)] = I_{AB} \leq I_{AB}(\mathrm{lim})$, where $I_{AB}(\mathrm{lim})$ is 24.5, 25, and 27.2 for the shallow and deep samples, respectively. In the lower redshift interval $0.4 < z < 0.7$ the wavelength corresponding to $4400(1 + z)$ lies shortward of the *I* band, but still we adopt the same threshold in $m[4400(1 + z)]$. This implies that some galaxies from the original I_{AB} limited samples are excluded from the LF since they have a red spectrum and consequently $m[4400(1 + z)]$ are fainter than our adopted threshold. We have in this way extracted a complete subsample of galaxies having a continuum magnitude threshold at 4400 Å in each redshift interval, independently of their color [assuming galaxies in this redshift interval to have $(R-I)_{AB} \geq 0$]. The same procedure has been adopted at higher z using the *K*-band selected sample. In the $1.3 < z < 3.5$ interval, the 4400 Å rest-frame wavelength is within or shortward of the *K* band, and the LF includes all the galaxies with $m[4400(1 + z)] = K_{AB} \leq K_{AB}(\mathrm{lim})$. Finally, the rest-frame absolute AB magnitude $M_B(\mathrm{AB})$ has been derived from the theoretical best-fit spectral energy distribution for each galaxy. The same fit provides the photometric redshift for each galaxy. In this way the *K*-correction has been derived for each galaxy from the interpolation between the observed magnitudes using the best-fit spectrum. Uncertainties in this interpolation produce on average small ($\lesssim$10%) errors in the rest-frame luminosities (Ellis 1997; Pozzetti et al. 2003). The rest-frame luminosity is derived without any correction for dust absorption.

To estimate the observed LF we have applied to our composite sample an extended version of the $1/V_{max}$ algorithm. Our combination of data from separate fields, with different magnitude limits, has been treated computing, for every single object, a set of effective volumes, $V_{max}(j)$, for each jth field under analysis. For a given redshift interval (z_1, z_2), these volumes are enclosed between z_1 and $z_{up}(j)$, the latter being defined as the minimum between z_2 and the maximum redshift at which the object could have been observed within the magnitude limit of the jth field.

The Poisson error in each LF magnitude bin was computed adopting the recipe by Gehrels (1986), valid also for small numbers. To compute the uncertainties in the LF due to the photometric z estimates, we assumed the typical rms found comparing photometric and spectroscopic z (where available) in the HDF-N and K20 samples. The adopted values range from $\sigma_z \sim 0.08$ at $z \sim 1$ to $\sigma_z \sim 0.16$ at $z \sim 3$ (Fontana et al. 2000; Cimatti et al. 2002a). We have generated from the original z photometric catalogs of *I*-selected or *K*-selected galaxies, a set of 50 catalogs of random photometric z using the above rms uncertainties to compute a set of 50 LFs. The derived fluctuations in each magnitude bin resulted to be smaller than Poissonian errors and have been added in quadrature. Due to the limited area of each survey, density fluctuations among the fields could be larger than Poissonian errors. For this reason both such uncertainties have been computed in each magnitude

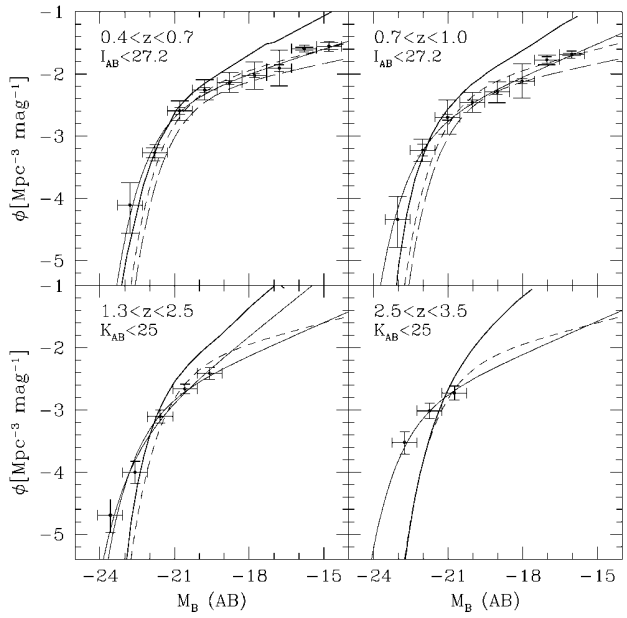

FIG. 1.—Blue luminosity function at various redshift intervals. Thick solid curve represents the LF predicted by the CDM model of Menci et al. (2002). Thin solid curve represents the Schechter fit to the unbinned data where the flatter slopes in the lower panels result from the fit with $\alpha = 1.44$. Short-dashed curve is the observed local LF from the Sloan survey (Blanton et al. 2001), where $M^* = -20.65$ has been derived from the g magnitudes adopting the following transformation $M_B^* = g^* + 0.32$ and scaling magnitude and normalization to $H_0 = 70$ km s^{-1} Mpc^{-1}. Long-dashed curve is the observed local LF from the 2dF survey. Larger vertical error bars come from the rms field-to-field variance, smaller bars from the Poissonian statistics.

bin of the LF at $z < 1$. At $z > 1$ the LF has been derived from the deep K-selected HDF-S sample, and thus only Poissonian errors have been computed.

A complementary way to study the evolution of the galaxy population is to apply a maximum-likelihood analysis assuming a Schechter parametric form ϕ for the LF (Sandage, Tammann, & Yahil 1979). In the case of our composite survey, which is based on j magnitude–limited fields, the maximum-likelihood Λ writes (Marshall et al. 1983)

$$\Lambda = \prod_{i=1}^{N} \frac{\phi(M_i)dz\,dM}{\sum_j \omega(j) \int_{z_1}^{z_2} (dV/dz)dz \int_{-\infty}^{M_{\rm lim}^j(z)} \phi(M)dM}, \qquad (1)$$

where $\omega(j)$ is the field area in steradians and N is the total number of objects considered in the composite sample. $M_{\rm lim}^j(z)$ is the absolute magnitude value corresponding, at the given redshift z, to the magnitude limit of the jth survey. The value of ϕ^* is then obtained simply imposing on the best-fit LF a normalization such that the total number of galaxies of the combined sample is reproduced.

4. THE EVOLUTION OF THE LF IN THE REST-FRAME 4400 Å BAND

The resulting LFs in different redshift intervals are shown in Figure 1, where in each panel the local (i.e., $z \lesssim 0.1$) observed blue LFs from the Sloan (Blanton et al. 2001) and 2DF (Norberg et al. 2002) surveys have been shown for comparison. First of all, we note that the LFs derived from the present I-selected composite sample up to $z = 1$ show little density evolution at the faint end with respect to the local values and the density remains approximately constant for $M_B(\mathrm{AB}) \sim -16$. A small underdensity is apparent at $0.7 < z < 1$ and $M_B(\mathrm{AB}) \sim -19$, but this appears to be of the same order as the differences between the two local LFs. At the bright end a brightening increasing with redshift is apparent with respect to the local LF. Indeed, as shown in Table 2, assuming a Schechter shape for the LF, the characteristic luminosity M_B^* increases from -21.3 to -21.9 in the range $z = 0.4$–1.

TABLE 2

PARAMETERS OF THE SCHECHTER FUNCTION FITS

z Range	α	M^*	ϕ_*	N
0.4–0.7	-1.33 ± 0.04	-21.33 ± 0.17	0.004	787
0.7–1	-1.44 ± 0.04	-21.88 ± 0.19	0.002	754
1.3–2.5	-1.80 ± 0.20	-22.37 ± 0.39	0.0007	96
1.3–2.5	-1.44	-21.87 ± 0.14	0.0017	96
2.5–3.5	-1.44	-22.30 ± 0.31	0.0015	42

It is interesting to compare our LF at $z \lesssim 1$ with that derived from the COMBO-17 survey (Wolf et al. 2003) based on photometric redshifts derived from a shallower sample ($R < 24$), but from a larger area of 1 deg^2. They derive for the overall sample characteristic luminosities $M_B^*(\mathrm{AB}) = -21$, -21.9, -22.2 (for $H_0 = 70$ km s^{-1} Mpc^{-1}) and slopes $\alpha = -1.1$, -1.6, and -2 at redshifts $z = 0.5$, 0.7, and 0.9, respectively. Formally, the slopes derived by the COMBO-17 survey are not statistically consistent with those obtained by our samples at similar z. However, given the significantly different limiting magnitudes of the two samples, it is difficult to compare with each other the two sets of slopes. In any case, both samples suggest a steepening of the LF coupled with an increase of M_B^* from $z \simeq 0$ up to $z \sim 1$.

At $z \sim 2$–3 our LF still shows a brightening with respect to the local value, which appears to be due to enhanced star formation activity for the brightest galaxies. This can be derived from Figure 2, where we plot the correlation existing between the observed rest-frame blue and the dereddened UV 1400 Å

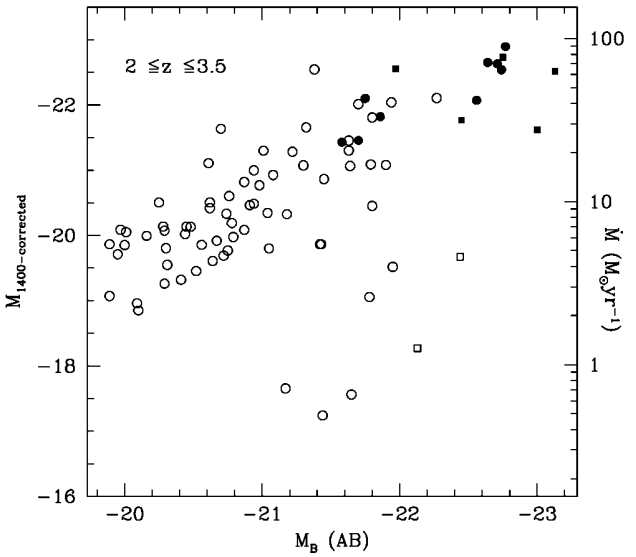

FIG. 2.—UV dereddened luminosity at 1400 Å rest frame vs. observed blue luminosity for galaxies in the HDF North (*squares*) and South (*circles*). A Small Magellanic Cloud extinction curve has been adopted. Using the Calzetti extinction curve increases the slope of the correlation reaching $M_{1400} \approx -25$ at $M_B \approx -22.5$. Filled symbols represent galaxies with spectroscopic redshifts. The corresponding star formation rate (*right axis*) has been derived using the Bruzual & Charlot (1993) code and assuming a Salpeter IMF.

luminosities derived from the spectral models fitting the NIR/optical colors of each K-selected galaxy. The median reddening for the galaxies in Figure 2 is $E(B-V) \sim 0.1, 0.2$ for SMC or Calzetti extinction curves, respectively, in agreement with Shapley et al. (2001). We have also checked the robustness of such a result using the correlation (Meurer, Heckman, & Calzetti 1999) between the rest-frame UV shape (derived from the observed optical colors) and the UV extinction, a procedure less dependent on the estimated age of the stellar population.

Thus, the correlation shown in Figure 2 implies that brighter blue galaxies have on average greater star formation activity. We note in this respect that 67%, 83%, and 67% of the brightest galaxies with $M_B(\mathrm{AB}) < -22$, $z < 1$, $1.3 < z < 2.5$, and $2.5 < z < 3.5$ have spectroscopic redshifts. Thus, the amount of brightening is measured with good accuracy despite the small number of sources involved at the bright end. We also note that some galaxies in Figure 2 contributing to the LF are clearly red with a small UV emission (see also Franx et al. 2003). It is difficult to argue about their nature (old or dust reddened) without spectroscopic information (see Franx et al. 2003). However, these red galaxies have in general $M_B > -22$, and so they have magnitudes of the order of M^* or fainter and do not affect the brightest end of the blue LF. They represent about 9% of the sample shown in Figure 2.

At the faint end of the LF, the Schechter slope α is not well constrained at these redshifts. The derived slope at $z = 1.3$–2.5 is $\alpha = -1.8$ and the related characteristic luminosity is $M_B^* \simeq -22.4$, but the uncertainties are large. Fixing the slope to the lower redshift value $\alpha = -1.4$ we derive a characteristic luminosity $M_B^* \sim -21.9$. Keeping the slope fixed a further brightening by about 0.4 mag ($M_B^* \sim -22.3$) is apparent in the redshift interval $z = 2.5$–3.5 (see Table 1). Similar results concerning the evolution of the blue LF and derived luminosity density have been obtained in the HDF-N NICMOS field by Dickinson et al. (Dickinson, Papovich, & Ferguson 2001; Dickinson et al. 2003). Our results are also consistent with the rest-frame V-band LF derived at $z \simeq 3$ by Shapley et al. (2001).

The above results are compared with the semianalytic model by Menci et al. (2002) describing the galactic merging histories in the framework of hierarchical models. The cooling, star formation, and supernovae (SNe) feedback of the galactic baryons are similar to other semianalytic models (Kauffmann et al. 1993; Somerville & Primack 1999; Cole et al. 2000). Stars are allowed to form from the cooled gas with rate $\dot{m}_* = (m_c/t_{\mathrm{dyn}})(v/200\ \mathrm{km\ s^{-1}})^{-\alpha_*}$, where t_{dyn} is the disk dynamical time. A mass $\Delta m_h = \beta m_*$ is returned from the cool to the hot gas phase due to the energy feedback by Type II SNe associated to m_*. The feedback efficiency is taken to be $\beta = (v/v_h)^{\alpha_h}$. The values adopted for the parameters are the same of Cole et al. (2000) and allow similar fits to the local B-band galaxy LF and the Tully-Fisher relation, as illustrated by Menci et al. (2002). However, our model also includes a physical prescription for the binary aggregations among satellite galaxies in common hosting halos, which provides a somewhat flatter luminosity function at all z. In comparing the observed LF with that predicted by our CDM model we did not correct the observed rest-frame luminosities for dust absorption but we have included the reddening effects in the model. The dust absorption has been assumed to be proportional to the disk surface density and metallicity as detailed in Menci et al. (2002). We adopted an SMC extinction curve; using a Milky Way or Calzetti extinction curves does not affect appreciably the resulting B-band luminosities.

The comparison shows two main features: (1) At the faint end of the LF the excess of predicted galaxies persists at all redshifts (see also Poli et al. 2001 and Cimatti et al. 2002b). This implies that some feedback could be effective in suppressing the star formation activity. However, since further increments of the SNe feedback would result in a local Tully-Fisher relation too faint when compared with the data, sources of feedback other than SNe should be investigated. An example is represented by the feedback provided by the diffuse ionizing UV background produced by QSOs. (2) At the bright end [$M_B(\mathrm{AB}) < -20$], the theoretical LFs show little evolution up to $z = 3.5$, resulting from the balance between the decrease with z of the number of massive objects and the increase of their star formation and hence of their blue luminosity. On the contrary, the observed LFs show an increasing brightening with redshift. Even if at $z < 1$ the predicted LFs are still consistent with this brightening, at $z > 1$ they fail to reproduce the observed number of bright galaxies. This discrepancy would then enlighten the lack in hierarchical models of sufficiently high star formation activity at $z = 2$–4, beyond the quiescent mode driven by the progressive refueling of the cold gas reservoir during galaxy merging and by the gradual cooling of the available hot gas. An additional burst mode triggered by galaxy interactions in common DM halos (e.g., Somerville & Primack 1999; Poli et al. 2001) could contribute to solve the problem. Indeed, the rate of interactions peaks in the above redshift interval (Menci et al. 2002).

REFERENCES

Bertin, E., & Arnouts, S. 1996, A&AS, 117, 393
Blanton, M. R., et al. 2001, AJ, 121, 2358
Bruzual A., G., & Charlot, S. 1993, ApJ, 405, 538
Casertano, S., et al. 2000, AJ, 120, 2747
Cimatti, A., et al. 2002a, A&A, 392, 395
———. 2002b, A&A, 391, L1
Cole, S., Lacey, C. G., Baugh, C. M., & Frenk, C. S. 2000, MNRAS, 319, 168
Connolly, A. J., Szalay, A. S., Dickinson, M., Subbarao, M. U., & Brunner, R. J. 1997, ApJ, 486, L11
Dickinson, M., Papovich, C., & Ferguson, H. C. 2001, in Deep Fields, ESO Astrophys. Symp., ed. S. Cristiani et al. (Garching: ESO), 68
Dickinson, M., Papovich, C., Ferguson, H. C., & Budavari, T. 2003, ApJ, 587, 25
Ellis, R. S. 1997, ARA&A, 35, 389
Ellis, R. S., Colless, M. M., Broadhurst, T. J., Heyl, J. S., & Glazebrook, K. 1996, MNRAS, 280, 235
Fernandez-Soto, A., Lanzetta, K. M., & Yahil, A. 1999, ApJ, 513, 34
Folkes, S., et al. 1999, MNRAS, 308, 459
Fontana, A., D'Odorico, S., Poli, F., Giallongo, E., Arnouts, A., Cristiani, S., Moorwood, A., & Saracco, P. 2000, AJ, 120, 2206
Franx, M., et al. 2003, ApJ, 587, L79
Gehrels, N. 1986, ApJ, 303, 336
Giacconi, R., et al. 2001, ApJ, 551, 624
Giallongo, E., D'Odorico, S., Fontana, A., Cristiani, S., Egami, E., Hu, E., & McMahon, R. G. 1998, AJ, 115, 2169
Kauffmann, G., White, S. D. M., & Guiderdoni, B. 1993, MNRAS, 264, 201
Labbé, I., et al. 2003, AJ, 125, 1107
Lilly, S., Tresse, L., Hammer, F., Crampton, D., & Le Fèvre, O. 1995, ApJ, 455, 108
Lin, H., Yee, H. K. C., Carlberg, R. C., Morris, S. L., Sawicki, M., Patton, D. R., Wirth, G., & Shepherd, C. W. 1999, ApJ, 518, 533
Marshall, H. L., Tananbaum, H., Avni, Y., & Zamorani, G. 1983, ApJ, 269, 35
Menci, N., Cavaliere, A., Fontana, A., Giallongo, E., & Poli, F. 2002, ApJ, 575, 18

Meurer, G. R., Heckman, T. M., & Calzetti, D. 1999, ApJ, 521, 64
Norberg, P., et al. 2002, MNRAS, 336, 907
Poli, F., Giallongo, E., Menci, N., D'Odorico, S., & Fontana, A. 1999, ApJ, 527, 662
Poli, F., Menci, N., Giallongo, E., Fontana, A., Cristiani, S., & D'Odorico, S. 2001, ApJ, 551, L45 (erratum 551, L127)
Pozzetti, L., et al. 2003, A&A, 402, 837
Sandage, A., Tammann, G. A., & Yahil, A. 1979, ApJ, 232, 352
Shapley, A., Steidel, C. C., Adelberger, K. L., Dickinson, M., Giavalisco, M., & Pettini, M. 2001, ApJ, 562, 95
Somerville, R. S., & Primack, J. R. 1999, MNRAS, 310, 1087
Vanzella, E., et al. 2001, AJ, 122, 2190
———. 2002, A&A, 396, 847
Wolf, C., Meisenheimer, K., Rix, H.-W., Borch, A., Dye, S., & Kleinheinrich, M. 2003, A&A, 401, 73
Zucca, E., et al. 1997, A&A, 326, 477